Job Plots

DOI: 10.1002/anie.201304157

Method of Continuous Variations: Applications of Job Plots to the Study of Molecular Associations in Organometallic Chemistry

*Joseph S. Renny, Laura L. Tomasevich, Evan H. Tallmadge, and David B. Collum**

Keywords:
aggregation · alkali metals · organometallics · reaction kinetics · transition metals

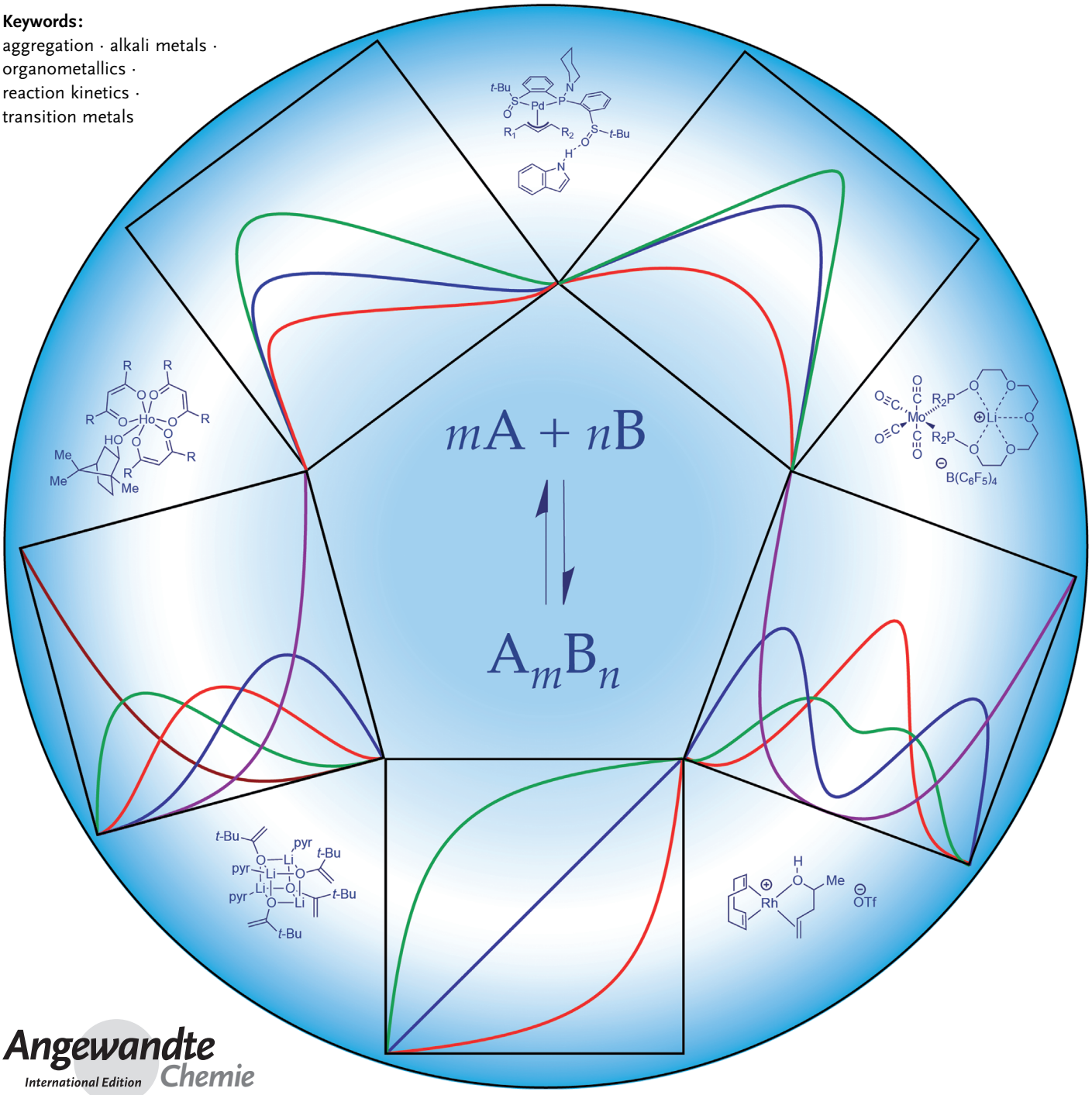

Angewandte International Edition Chemie

Applications of the method of continuous variations (MCV or the Method of Job) to problems of interest to organometallic chemists are described. MCV provides qualitative and quantitative insights into the stoichiometries underlying association of m molecules of ***A*** *and n molecules of* ***B*** *to form* $\mathbf{A}_m\mathbf{B}_n$*. Applications to complex ensembles probe associations that form metal clusters and aggregates. Job plots in which reaction rates are monitored provide relative stoichiometries in rate-limiting transition structures. In a specialized variant, ligand- or solvent-dependent reaction rates are dissected into contributions in both the ground states and transition states, which affords insights into the full reaction coordinate from a single Job plot. Gaps in the literature are identified and critiqued.*

From the Contents

1. Introduction

Molecular association is the bedrock of simple acid-base equilibria, metal ion solvation, transition metal coordination, enzyme catalysis, host-guest complexation, molecular sensing, and dissolution. Limited reflection reveals chemistry that does not involve some form of molecular association is indeed exceptional.

How are the existence, strength, and stoichiometry of such associations detected? At the start of the 20th century a number of chemists began addressing these questions using graphical methods. Following several seminal contributions largely lost in dusty archives,[1] a 1928 paper published by Paul Job[2] captured the imagination of the chemical community. As part of a thorough and scholarly study of ion associations, Job showed that plotting UV absorption versus mole fraction, X_A, of $Tl(NO_3)$ in $Tl(NO_3)/NH_3$ mixtures afforded a plot akin to the idealized depiction in Figure 1. A maximum in the curve at $X_A = 0.5$ implicates a 1:1 molecular association. The graphical output of what had previously been referred to as the method of continuous variations (MCV)[3,4] became known as a Job plot.

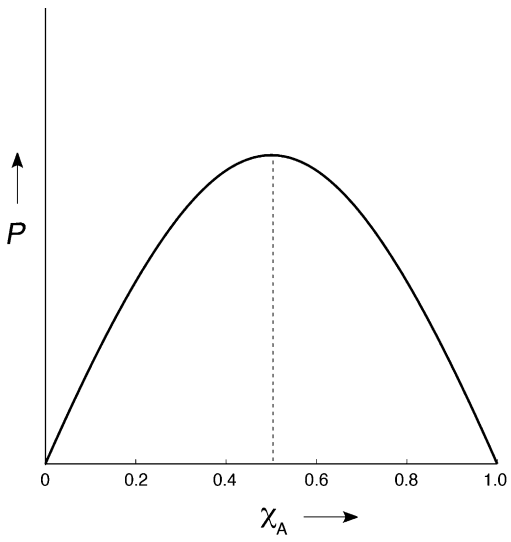

Figure 1. Rendition of the simplest form of a Job plot deriving from a 1:1 complexation manifesting a maximum in physical property, *P*, at mole fraction of **A**, X_A, of 0.5 [Eq. (1)].

$$Tl(NO_3) + NH_3 \rightleftharpoons H_3N{-}Tl(NO_3) \quad (1)$$

During studies of organolithium chemistry, we have found Job plots to be remarkably versatile with varied applications. Nonetheless, casual observations suggested that organometallic chemists—despite an acute interest in molecular associations not the least of which being metal-ligand interactions—have shown relatively little interest in Job plots. In 1973 Hartley and Wagner[5] noted this paucity of organometallic examples, which persists to this day.

We present results from a survey of over 6500 papers culled from all areas of chemistry and biochemistry in which MCV was applied in some form. The literature search protocol is described at the end. Although the literature search was our best effort to be comprehensive, we initially intended this review to be a narrative, not an exhaustive treatise, with the goal of underscoring the untapped potential of MCV in organometallic chemistry. We subsequently discovered that examples of Job plots in organometallic chemistry are so rare that a comprehensive survey proved easier than a cohesive narrative. We may have missed a few applications, but surely not many. A disproportionate number of examples from organolithium chemistry reflects that discipline's willingness to embrace the method rather than our own predilections. We also include select applications that are more inorganic than organometallic chemistry to fill in gaps and illustrate salient ideas.

We begin with a discussion of Job plots in their simplest forms to introduce the qualitative features of the method for

[*] Dr. J. S. Renny, L. L. Tomasevich, E. H. Tallmadge, Prof. D. B. Collum
Department of Chemistry and Chemical Biology
Baker Laboratory, Cornell University
Ithaca, New York, NY 14853–1301 (USA)
E-mail: dbc6@cornell.edu
Homepage: http://collum.chem.cornell.edu/

the nonspecialist irrespective of discipline (section 2). This overview is followed by a brief discussion of fitting protocols to provide access to the highly limited literature on curve fitting (section 3). Section 4 discusses applications of potential interest to organometallic chemists with subsections including simple examples of observable binding (4.1 and 4.2), studies of complex ensembles (4.3), and applications of MCV to reaction kinetics (4.4). Section 4.5 concludes with a strategy for examining observable associations and associations corresponding to transition structures, all in a single Job plot.

The review relies on computed (simulated) Job plots owing to the widely variable style and quality of data in the original papers. We also do not shy away from editorial comments about gaps in the literature, occasionally interjecting how rarely a particular advantage of MCV has been exploited. All such statements of frequency can be implicitly prefaced with, "From a survey of over 6500 applications of Job plots…"

2. What is a Job Plot?

Imagine the binary complexation in Equation (2). Complexation could be probed by holding the concentration of **B** fixed, systematically varying the concentration of **A**, and monitoring a physical property, *P*, that serves as a proxy for the concentration of binary complex **AB** (Figure 2). The asymptotic approach to complete conversion to **AB** is often referred to as saturation.[6] The curvature provides the relative stoichiometries of **A** and **B** and even a quantitative measure of binding (K_{eq}) but only to the most discerning eye or with the aid of a nonlinear least squares fit.[6] An analogous plot could be obtained by holding the concentration of **A** constant and varying the concentration of **B**. Taken together, the two plots provide insights into the relative stoichiometries of **A** and **B**.

$$\mathbf{A} + \mathbf{B} \overset{K_{eq}}{\rightleftharpoons} \mathbf{AB} \qquad (2)$$

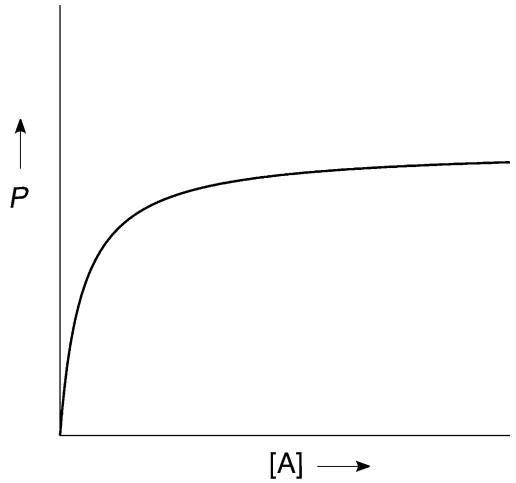

Figure 2. Plot showing saturation indicative of full conversion of **A** to **AB** with increasing concentration of **A** [Eq. (2)].

Instead of varying the concentration of one component at a time, MCV holds the total concentration of added **A** and **B** constant and varies their relative proportions.[7] The units on the *x* axis morph from concentration to mole fraction of **A** or **B** ($X_{\mathbf{A}}$ or $X_{\mathbf{B}}$ such that $X_{\mathbf{A}} = [\mathrm{A}]/\{[\mathrm{A}]+[\mathrm{B}]\} = 1-X_{\mathbf{B}}$). *The use of mole fraction or its equivalent along the x axis is shared by all Job plots.* The result is a very different view of the same equilibrium (Figure 3).[8]

David B. Collum received a bachelor's degree in biology from the Cornell University College of Agriculture and Life Sciences in 1977. After receiving a Ph.D. in 1980 from Columbia University working with Professor Clark Still, he returned to the Department of Chemistry at Cornell, where he is now a Professor of Chemistry. His previous work at Cornell addressed topics in natural products synthesis and organotransitionmetal chemistry but has focused on understanding organolithium structure and mechanism for several decades.

Laura L. Tomasevich was born in Pittsburgh. She received a bachelor's degree in chemistry in 2008 from Washington & Jefferson College, where she investigated novel heterocyclic rearrangements. She is currently completing her doctoral studies at Cornell University under the guidance of Prof. David B. Collum, studying the solution structures of enolates and phenolates.

Joseph S. Renny was born in London in 1982. He received his M.Sci. in chemistry (2006) from the University of Bristol and obtained his Ph.D. (2010) on the mechanism and catalysis of the Newman–Kwart rearrangement under the supervision of Prof. Guy C. Lloyd-Jones. He conducted postdoctoral studies under Prof. David Milstein at the Weizmann Institute, Israel. In the fall of 2011 he moved to his present position as a postdoctoral associate with Professor David B. Collum at Cornell University.

Evan H. Tallmadge is from Colchester, Vermont, and received his BS in Biochemistry from Stonehill College in 2010, researching under Prof. Marilena F. Hall. Upon graduation, he began his doctoral work at Cornell University under the tutelage of Prof. David B. Collum exploring the solution structures of lithiated Evans' oxazolidinone enolates and the relationship between their aggregation and enantioselectivity.

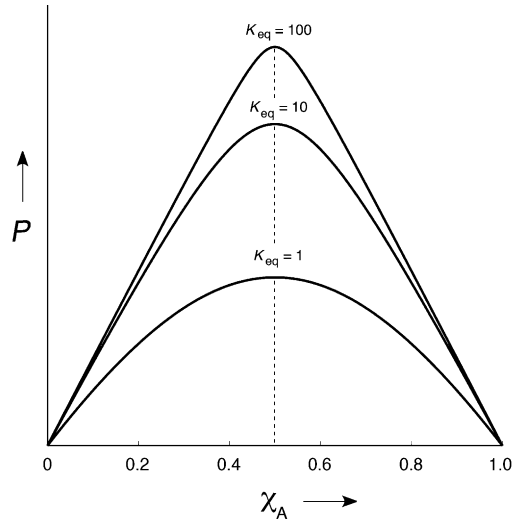

Figure 3. Job plots corresponding to the binary 1:1 combination [Eq. (2)] using a normalized physical property, P, and $K_{eq}=1$, $K_{eq}=10$, and $K_{eq}=100$.

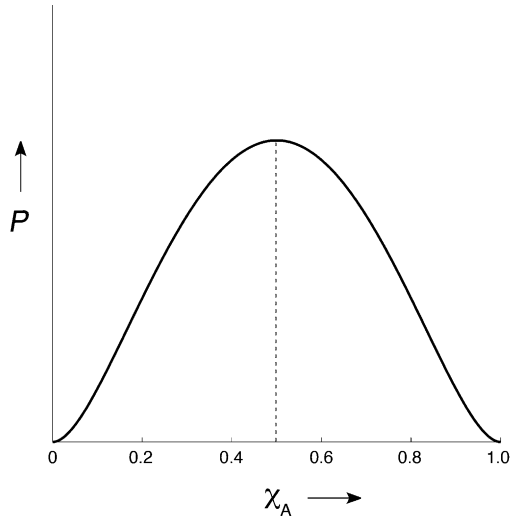

Figure 4. Job plots corresponding to the binary 2:2 combination.

The simplicity and power of the Job plot are compelling. The most common dependent variable for the y axis is a UV-Vis absorbance,[9] but any property that correlates linearly with the concentration of **AB** suffices, including kinetics,[10] conductivity,[11] permittivity,[12] NMR spectroscopy,[7b,13] calorimetry,[14] circular dichroism,[15] circularly polarized luminescence,[16] gravimetric titration,[17] relaxivity,[18] and melting point depression.[19] MacCarthy has described a relatively untested but provocative protocol for collecting the entire data set of a Job plot in a single automated experiment.[20]

Even without calibration of the molar response of **AB**, the shape of the curve provides qualitative insight into K_{eq} (Figure 3): strong binding ($K_{eq} \gg 1$) affords a more angular plot approaching the shape of a perfect triangle in the limit, whereas a more balanced equilibrium affords gentle curvature. The position of the maximum at $X_A = 0.5$, identified by inspection in the simplest analysis, provides the 1:1 stoichiometry of an $\mathbf{A}_m\mathbf{B}_n$ complex ($m=n$). The position of the maximum does *not* distinguish 1:1, 2:2, and other n:n relative stoichiometries, but subtle changes in curvature can provide clues of higher-order complexes. A 2:2 stoichiometry [Eq. (3)] affords a symmetric curve with a very subtle bell shape that can be difficult to discern experimentally (Figure 4).[21]

$$2\,\mathbf{A} + 2\,\mathbf{B} \rightleftharpoons \mathbf{A_2B_2} \tag{3}$$

Although the literature is dominated by examples of binary complexation, Job plots showing $\mathbf{AB_2}$ stoichiometries are prevalent [Eq. (4)].[22] These Job plots display maxima at $X_A = 0.33$ (Figure 5). The sigmoidal curvature on the right-hand side of the curve also attests to the stoichiometry, but it can be difficult to observe experimentally.

$$\mathbf{A} + 2\,\mathbf{B} \overset{K_{eq}}{\rightleftharpoons} \mathbf{AB_2} \tag{4}$$

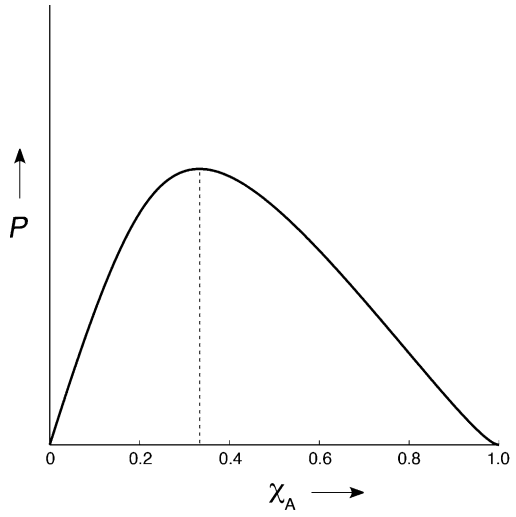

Figure 5. Job plot showing a 2:1 binding stoichiometry [Eq. (4)] for an $\mathbf{AB_2}$ complex.

3. Mathematics and Fitting

The merits of MCV are its simplicity. We estimate, for example, that only 3–5% of Job plots—maybe 100 examples—include any form of computer-aided fit. There are, however, arguments for at least minimally understanding the capabilities of fitting protocols. Ironically, some of the most impressive and ambitious examples of such fits were published in the era pre-dating personal computers and user-friendly statistical programs capable of routine least-squares analyses. (We have provided 30 minute, self-guided tutorials for two standard statistical packages.)[23]

Equation (5) describes a fit to the binary equilibrium in Equation (2) relating observable P versus X_A, affording K_{eq} as an adjustable parameter.[24] The odd mathematical form stems from the need to use the quadratic equation to solve for [**AB**].

Although some authors measure the molar response corresponding to the maximum (P_{max}) of the **AB** complex, the molar response, c, can be determined as an adjustable parameter.[24] If the fit fails, the chemistry may not be as simple as presumed. The quality of the fit tests the veracity of the chemical model: if it does not fit you must acquit. We provide examples below in which subtle curvatures foreshadow greater complexity.

$$[AB] = \frac{1 + cK_{eq} - \sqrt{1 + 2cK_{eq} + [cK_{eq}(1 - 2X_A)]^2}}{2K_{eq}} \quad (5)$$

Notable efforts to quantitate MCV have been provided by Bühlmann,[25] Huang,[26] Olivera,[27] Hirose,[28] and others[29] with varying degrees of clarity and detail.[30] Bühlmann analyzes diverging curvatures arising from 1:1 and 2:2 stoichiometries [Eq. (2) and (3)] that would easily be missed without the aid of fitting protocols (Figure 4). Bühlmann also distinguishes simple associations from displacements [Eq. (6)] in which complexation affords **AB** plus a byproduct, **D**.[25] The underlying mathematics and data workup is fairly specialized. If a rigorous fit is needed, "flooding" the reaction with excess **D** akin to pseudo-first-order kinetics[6] to hold its concentration constant suffices.

$$\mathbf{A} + \mathbf{B} \rightleftharpoons \mathbf{AB} + \mathbf{D} \quad (6)$$

Higher-order complexations, including the 2:1 and 2:2 stoichiometries, call for more sophisticated mathematical treatments and caution. The general depiction of the formation of any $\mathbf{A}_m\mathbf{B}_n$ complex is illustrated in Equation (7). A deceptively simple expression is described by Equation (8).[31,32] Unfortunately, Equation (8) is only valid in the limit that $\mathbf{A}_m\mathbf{B}_n$ does not build up appreciably, which is most likely found in steady-state solution kinetics.[32] The problem with Equation (8) stems from the fact that a build up of $\mathbf{A}_m\mathbf{B}_n$ causes the concentrations of **A** and **B** to become unknowns. Nonetheless, Equation (8) will afford a credible fit if the equilibria do not deviate markedly from statistical and provided one is not interested in extracting the value for K_{eq}. The rigorous solution—the Rosetta Stone of Job plots that fits any and all stoichiometries—is described by Equation (9) and is discussed in detail by Asmus and Klausen.[8,33] (c in Eq. (9) corresponds to the maximum reading, P_{max}.) Equation (9), an implicit equation that does not lend itself to simple factoring, demands somewhat advanced numerical methods. The mathematical skills presumed by the authors who apply these methods often exceed those of many practitioners.[25] We close this section, however, by noting that none of this detailed mathematical analysis is required to reap the enormous benefits offered by MCV: you can simply plot points if you wish.

$$m\,\mathbf{A} + n\,\mathbf{B} \rightleftharpoons \mathbf{A}_m\mathbf{B}_n \quad (7)$$

$$[A_mB_n] = c(X_A)^m(1 - X_A)^n \quad (8)$$

$$\frac{1}{K_{eq}}[A_mB_n] = (cX_A - m[A_mB_n])^m(c(1 - X_A) - n[A_mB_n])^n \quad (9)$$

4. Job Plots in Organometallic Chemistry

MCV is used in all areas of chemistry to establish the stoichiometry of an observable complexation of two species. Oddly enough, however, organometallic chemistry is poorly represented. We begin with several simple examples.

4.1. Simple Observable Associations: Transition Metals and Lanthanides

During studies of Rh^I complexation with homoallylic alcohols [Eq. (10)], Anslyn and co-workers[34] used MCV to detect binary complexation (1:1 stoichiometry), forming chelate **1**. The complexes were monitored using ^1H NMR spectroscopy. The equilibrium constants were ascertained through independent titration experiments rather than by fitting the Job plot.

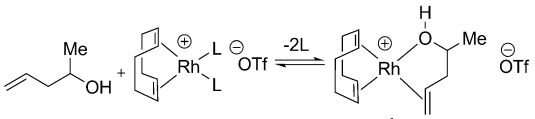

L,L = CH_3CN or η^2-cyclooctadiene

1 (1:1) (10)

Kraft and co-workers[35] used palladium(IV)tetrachloride carbene complex **2** as a pre-catalyst for the chlorination of alkenes and benzylic C–H bonds that is activated by a chloride source. Proton NMR studies in conjunction with MCV demonstrated that the catalytically active chlorinating agent is a 1:1 complex of **2** and chloride ion. Once again, the binding constant was determined through separate measurements rather than by fitting the Job plot. Complexation of the chloride to the imidazolium backbone via hydrogen bonding was proposed.

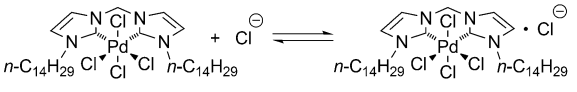

2 **3** (1:1) (11)

During studies on Lewis acid-mediated tungsten-catalyzed alkyne polymerizations, Baibich and co-workers[36] confirmed the formation of a 1:1 adduct of a tungsten alkene-carbene complex with triethylaluminum [Eq. (12)]. IR and NMR spectroscopies showed coordination to the carbonyl oxygen.

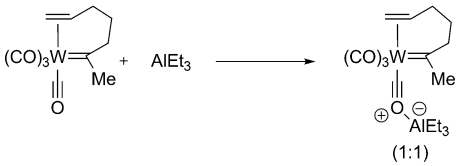

(12)

Brittain and co-workers[16] used circularly polarized luminescence to study the association of (*R*)-*p*-hydroxyphenylglycine and (*S*)-tyrosinol to lanthanides [Eq. (13)] and relied on MCV to confirm 1:1 complexes. Noting the initial concentrations and the mole fraction of uncomplexed [Tb(dpa)$_3$]$^{3-}$ (dpa = dipicolinate), they showed that the equilibrium constant was greater at high pH than at low pH, which suggested competing inner versus outer sphere association.

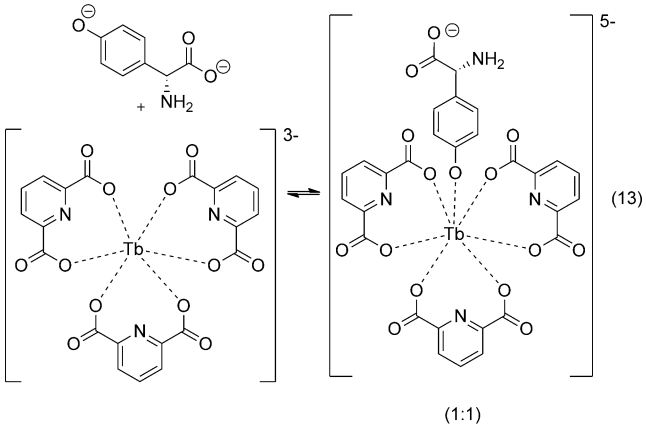

(13)

During studies on the Pd-catalyzed allylic alkylation of indoles, Liao and co-workers[37] developed a catalyst system capable of hydrogen bonding with indole substrates [Eq. (14)]. MCV confirmed the 1:1 catalyst-substrate complexation.

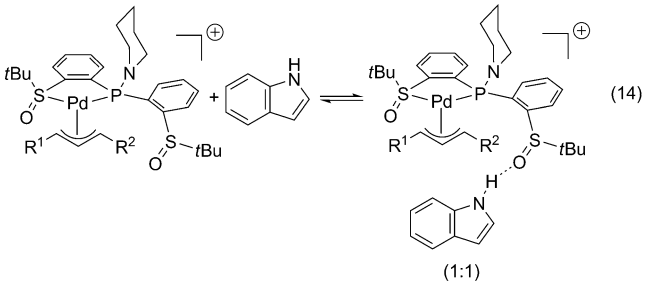

(14)

Studies of the oxidation of alcohols by OsO_4 in the presence of sodium hydroxide [Eq. (15)] by Gerber and co-workers[38] detected a comproportionation between *cis*-[Os^{VIII}O$_4$(OH)$_2$]$^{2-}$ (**4**) and *cis*-[Os^{VI}O$_2$(OH)$_4$]$^{2-}$ (**5**) that affords two [Os^{VII}O$_3$(OH)$_3$]$^{2-}$ [Eq. (16)], which is incapable of oxidizing aliphatic alcohols. A Job plot derived from Os^{VIII}/Os^{VI} mixtures at two absolute concentrations analyzed with UV/Vis spectroscopy confirmed the 1:1 comproportionation and afforded equilibrium constants and molar extinction coefficients for all three species. The authors also used MCV to calculate a distribution for each osmium species and excluded a 2:2 complex because of the parabolic rather than bell-shaped Job plot (see Figure 4).

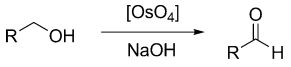

(15)

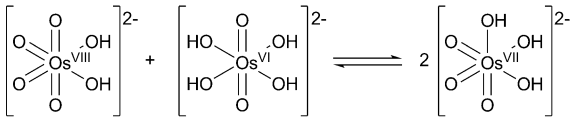

(16)

Cyclic voltammetry of mixed-metal complex **7** revealed a reversible one-electron oxidation. Colbran and co-workers[39] used MCV with UV monitoring to show that reaction of **7** with bromine [Eq. (17)] provided a 2:1 complex.

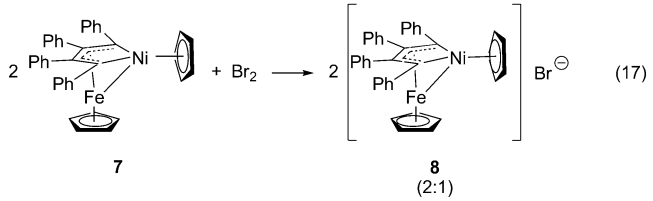

(17)

During studies of the self assembly in Equation (18), Sieklucka and co-workers[40] confirmed the 2:2 Co:W stoichiometry and used least-squares fitting to extract the binding constant. Notably, the least-squares fit also provided the molar absorption coefficients of the aggregated species as an adjustable parameter, which has only been done in a few cases throughout the vast MCV literature.

Sulfur dioxide has been used to model CO complexation to rhodium and iridium hydroformylation catalysts.[41] Salaita et al.[42] used MCV to show that sulfur dioxide and a rho-

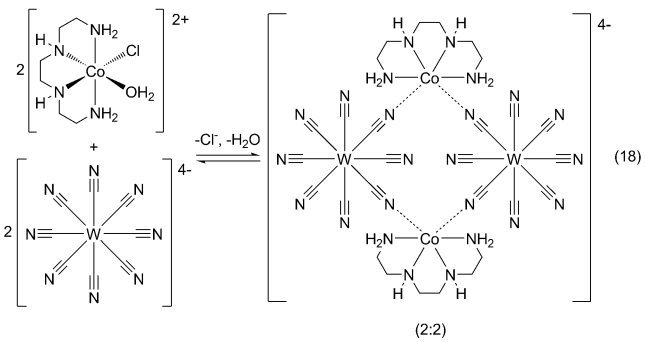

(18)

dium(I) carbonyl complex afford an observable 1:1 complex at short reaction times [Eq. (19)] and a 2:1 SO_2:Rh complex after prolonged reaction times [Eq. (20)]. The slow second complexation afforded a second Job plot. Both plots displayed angularity consistent with large binding constants (see Figure 3).

$$[Rh(CO)_2Cl_2]^- + SO_2 \xrightarrow[25\ ^\circ C]{3\ h} [Rh(SO_2)(CO)_2Cl_2]^- \quad (1{:}1) \qquad (19)$$

$$[Rh(CO)_2Cl_2]^- + 2SO_2 \xrightarrow[25\ ^\circ C]{48\ h} [Rh(SO_2)_2(CO)_2Cl_2]^- \quad (2{:}1) \qquad (20)$$

Duddeck and co-workers[43] found that adducts of dirhodium complex **10** prepared from chiral Mosher's acid and selenoether **9** cause the methoxy moieties on Mosher's acid [Eq. (21)] to display unique chemical shifts for the uncomplexed ethers, two diastereomeric monocomplexed ethers, and the three diastereomeric dicomplexed ethers (**11a–c**). Under conditions of rapid exchange, MCV confirmed the 2:1 stoichiometry of **11a–c**.

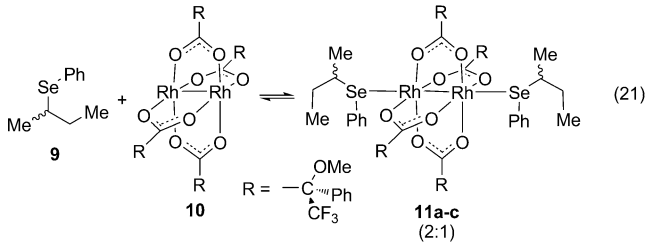

(21)

Hartley and Wagner[5] investigated the ligation of 1-hexene and 1-octene to solutions of $Na_2[Pd_2Cl_6]$ in acetic acid and detected two complexes. Monitoring the complexation with UV/Vis (265–320 nm) revealed the existence of $Na[Pd_2Cl_5(olefin)]$ at low olefin concentration, which MCV confirmed to be a 1:1 complex. Analogous measurements at 370–410 nm revealed the corresponding net 2:1 Pd_2Cl_4-(1-octene)$_2$ complex.

$$Na_2[Pd_2Cl_6] + \text{olefin} \xrightleftharpoons{-\ NaCl} Na[Pd_2Cl_5(olefin)] \quad (1{:}1) \qquad (22)$$

$$Na[Pd_2Cl_5(olefin)] + \text{olefin} \xrightleftharpoons{-\ NaCl} Pd_2Cl_4(olefin)_2 \quad (1{:}2) \qquad (23)$$

olefin = C_4H_9 or C_6H_{11}

Yamamoto and co-workers[44] studied electron transfer within an ion-paired dinuclear porphyrin species prepared from cobalt complexes ligated by TMPyP and TPPS.

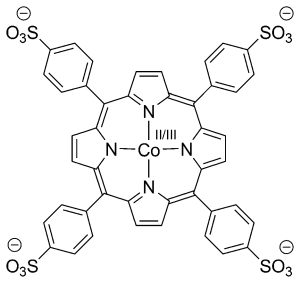

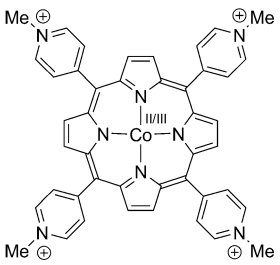

The putative ion-paired sandwiches could effect a four-electron reduction of oxygen. The cobalts were in the Co^{II} or Co^{III} oxidation states [Eqs. (24)–(26)], and the complexations were monitored by UV spectroscopy. MCV with least-squares fits of the experimental data afforded the stoichiometries (1:1) and dissociation constants ($K_{eq(1)}$–$K_{eq(3)}$). Dinuclear pairs form except with the Co^{III}-Co^{III} system [Eq. (26)], where further aggregation generates low concentrations of a trinuclear (2:1) sandwich [Eq. (27)].

$$[Co^{II}TPPS]^{4-} + [Co^{II}TMPyP]^{4+} \xrightleftharpoons{K_{eq(1)}} [Co^{II}TPPS\text{-}Co^{II}TMPyP]^0 \quad (1{:}1) \qquad (24)$$

$$[Co^{III}TPPS]^{3-} + [Co^{II}TMPyP]^{4+} \xrightleftharpoons{K_{eq(2)}} [Co^{III}TPPS\text{-}Co^{II}TMPyP]^+ \quad (1{:}1) \qquad (25)$$

$$[Co^{III}TPPS]^{3-} + [Co^{III}TMPyP]^{5+} \xrightleftharpoons{K_{eq(3)}} [Co^{III}TPPS\text{-}Co^{III}TMPyP]^{2+} \quad (1{:}1) \qquad (26)$$

$$[Co^{III}TPPS\text{-}Co^{III}TMPyP]^{2+} + [Co^{III}TPPS]^{3-} \xrightleftharpoons{K_{eq(4)}} [Co^{III}TPPS\text{-}Co^{III}TMPyP\text{-}Co^{III}TPPS]^- \quad (2{:}1) \qquad (27)$$

Catton et al.[45] investigated the complexation of chiral organic molecules (**13–15**) with NMR shift reagent, [Ho(tmhd)$_3$] (**12**) to correlate induced chemical shifts with independently measured binding. In one of the earliest and particularly scholarly applications of MCV using nonlinear least squares fit, the stoichiometries and equilibrium constants of binding were ascertained using UV-Vis showing 1:1 complexation [Eq. (28)]. The authors noted that control experiments (including simulations) showed that a 1:2 complex would not necessarily be readily detected from the Job plot in the event of coincident extinction coefficients of the 1:1 and 1:2 complexes.

The coordination of Li^+ cations to a molybdenum-based metallacrown ether was investigated with ^{31}P NMR spectroscopy [Eq. (29)].[46] A Job plot revealed 1:1 binding. This mixed-metal case represents an excellent transition to the next category—MCV applied to complexation of main group chemistry.

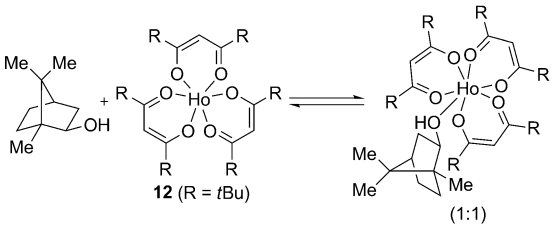

(28)

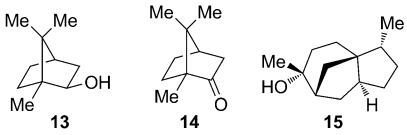

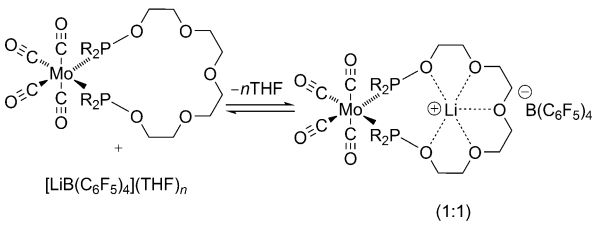

(29)

4.2. Simple Observable Associations: Main Group Metals

One finds a seemingly disproportionate use of MCV by main group organometallic chemists. This may arise from a relatively greater emphasis on solvation, aggregation, and Lewis acid-base complexation or simply from different cultural biases.

Taylor and co-workers[47] reported that borinic esters can effect the regioselective monofunctionalization of diols. Rate studies combined with MCV determined that the resting state in the catalytic cycle was 1:1 complex **18** constituted from diol **16** and borinic acid **17** [Eq. (30)].

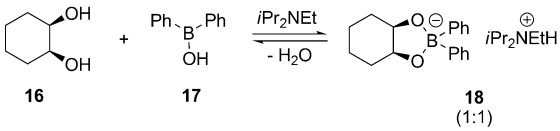

(30)

Organolithium chemists have gravitated toward MCV, possibly owing to their requisite obsession with aggregation and solvation. Tokitoh and co-workers[48] isolated unsolvated lithium diketiminate **19** as a crystalline solid. MCV revealed that solvation by tetrahydrofuran (THF) affords a 1:1 complex [Eq. (31)], presenting a direct measure of the primary solvation shell. The equilibrium constant was determined independently through a titration experiment rather than via the Job plot.

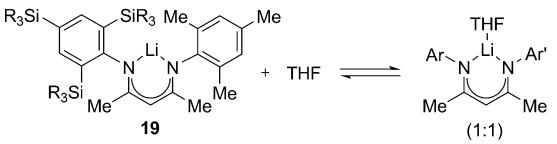

(31)

In a more complex variant, Jacobsen and co-workers[49] investigated the primary-solvation shell of lithium pinacolate (**20**) using ^{1}H NMR spectroscopy in conjunction with MCV [Eq. (32)]. THF binding to enolate hexamer **20** affords a 4:4 adduct (1:1 per subunit), whereas pyridine binding affords a sub-stoichiometric trisolvated tetramer (4:3). The failure of pyridine to fully solvate the putative cubic tetramer seems surprising in light of the efficacy of pyridine as a ligand, but the conclusions were amply supported by colligative measurements and a crystal structure of trisolvate **22**. An important point here is also a recurring theme within the forthcoming discussions of lithium salts: the Job plot was reported using mole fraction of the enolate subunit rather than the aggregate, affording maxima at the indicated stoichiometries. In this case, potentially confounding curvatures resulting from serial solvation were probably obscured by averaging of the chemical shift.

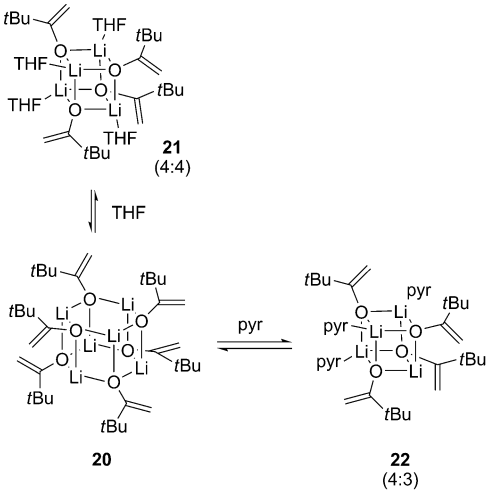

(32)

Lithium amide dimer **23** and *n*BuLi in neat THF generate mixed dimer **24** (1:1 stoichiometry by subunit) as confirmed by Williard and co-workers[31] using MCV and NMR spectroscopy. By contrast, reaction in neat toluene affords 1:3 tetramer **25**. The studies are notable in that nonlinear least squares fit to Equation (8) (albeit pre-ordained to afford a statistical curve as discussed in section 3) is excellent. Normalizing the mole fraction to the subunits rather than to the aggregates (normality rather than molarity) negates the effect of lithium amide and *n*-butyllithium aggregation numbers on the shape of the Job plot, rendering the position of the maxima intuitive. When the aggregation states of the complexing agents are unknown, this normalization is imperative.

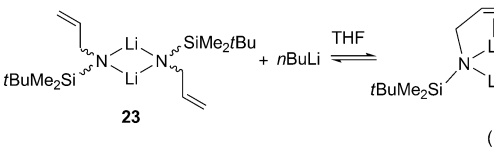

(33)

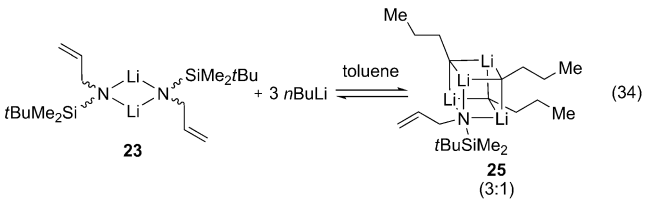

(34)

Brown and co-workers[12] investigated the solvation of ethyllithium (EtLi) hexamer by triethylamine [Eq. (35)]. The change in dielectric constant of the mixture accompanying formation of disolvated ethyllithium dimer was monitored. When the mole fraction is normalized per subunit, the maximum occurs at $X_A = 0.5$, showing the 1:1 Et_3N-Li ratio. Although we are somewhat surprised by the dimer assignment, this represents one of the earliest measurements of a lithium ion solvation number.

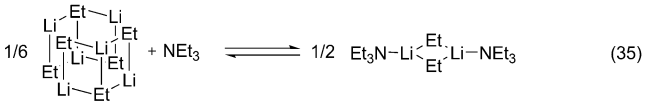

(35)

Reaction of diisobutylaluminum hydride with triisobutylaluminum shows a strongly temperature-dependent aggregation (Scheme 1).[50] Solution NMR experiments and MCV led Eisch and co-workers to assign the stoichiometries. Three Job plots corresponding to the three aggregates were necessarily created independently because of the temperature dependence. In the next section, we consider the role of MCV in characterizing complex ensembles.

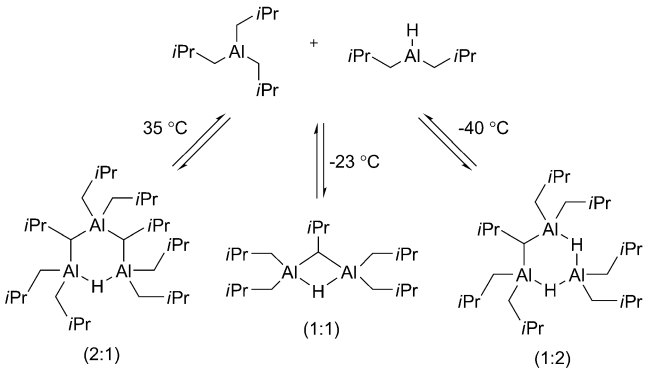

Scheme 1.

4.3. Complex Ensembles

Eisch's investigations of dialkylaluminums represents a study of what we call ensembles. In one of the simplest incarnations, association of $\mathbf{A_2}$ and $\mathbf{B_2}$ to form $2\mathbf{AB}$ [Eq. (36)] affords a statistical distribution (Figure 6). The more generalized ensemble is illustrated in Equation (37). This example is potentially important given that many main group metal alkyls are prone to aggregation.

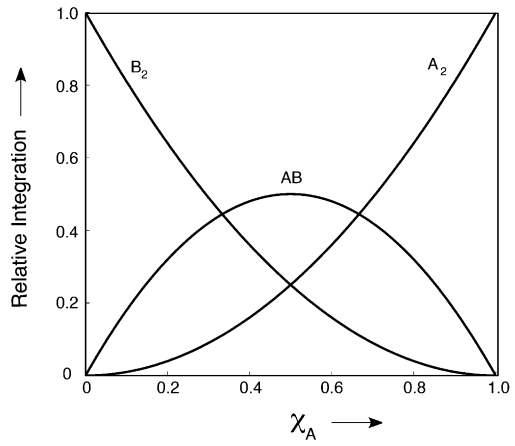

Figure 6. Job plot showing the statistical variant of the dimer ensemble in Equation (36).

$$\mathbf{A_2} + \mathbf{B_2} \rightleftharpoons 2\mathbf{AB} \tag{36}$$

$$\mathbf{A}_n + \mathbf{B}_n \rightarrow \mathbf{A}_n + \mathbf{A}_{n-1}\mathbf{B_1} + \mathbf{A}_{n-2}\mathbf{B_2} + \ldots \mathbf{B}_n \tag{37}$$

In one of the earliest and most thorough studies of ensembles using MCV, Weingarten and Van Wazer[51] monitored $[Ti(OR)_m(NR'_2)_n]$ mixed alkoxide-amide complexes using ^{1}H NMR spectroscopy [Eq. (38)].

$$\begin{aligned} Ti(OR)_4 \rightleftharpoons (R_2N)Ti(OR)_3 \rightleftharpoons (R_2N)_2Ti(OR)_2 \rightleftharpoons \\ (R_2N)_3Ti(OR) \rightleftharpoons (R_2N)_4Ti \end{aligned} \tag{38}$$

The resulting Job plot is similar to the statistical rendition in Figure 7. The symmetries of the aggregates and stoichiometries indicated by the positions of the maxima are consistent with *tetrasubstituted* complexes. Although the curves were calculated by manually adjusting K_{eq} to maximize superposition on the data, exploiting the mathematical framework first developed by Groenweghe and co-workers[52] was a seminal effort. Similar mathematical treatments were subsequently developed by Gil and Oliveira[27] and Collum

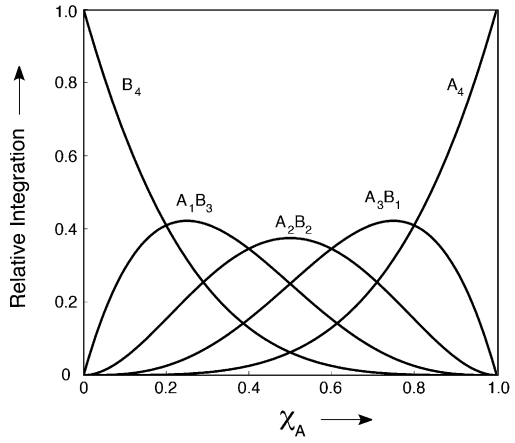

Figure 7. Job plot showing the statistical variant of the tetramer-based ensemble [Eq. (37), $n = 4$].

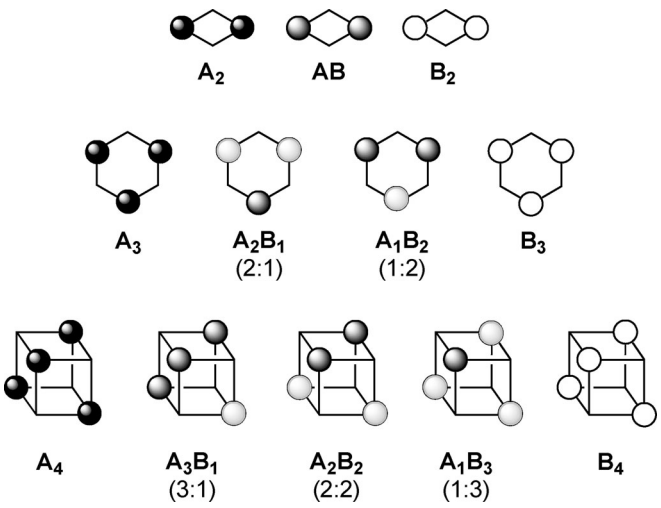

Figure 8.

and co-workers,[53] which in conjunction with modern computers and software packages bring the fits within reach of the general practitioner.

Most of the experimentally monitored ensembles reported to date are alkali metal salts. Figure 8, for example, illustrates magnetically inequivalent positions with mixed dimers, trimers, and tetramers of alkali metals. In 1993, Chabanel and co-workers[54,55] showed that a lithium acetylide and lithium isothiocyanate in THF afforded a Job plot with a maximum at $X_A = 0.50$ consistent with the formation of a mixed dimer [Eq. (39)].

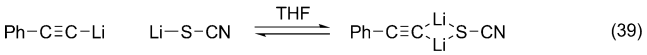

(39)

In triethylamine, by contrast, an ensemble of tetramers (Scheme 2) was evidenced by a non-statistical analog of the tetramer ensemble depicted in Figure 7 that displays the expected maxima at X_A of 0.25, 0.50, and 0.75.[54] In this case, omission of the homoaggregates from their Job plot attests to the authors' emphasis on mixed aggregation.

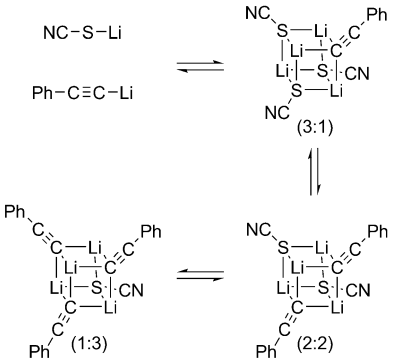

Scheme 2.

In 1972, Novak and Brown[56] monitored MeLi/LiI mixtures versus mole fraction using ^{6}Li NMR spectroscopy. They detected a tetramer ensemble (see Figure 8) but stopped short of generating a Job plot. In 2003, however, Maddaluno and co-workers[57] characterized analogous MeLi/LiBr mixtures and presented the data in the format of a Job plot analogous to Figure 7, albeit with detectable departures from statistical.

Kissling and Gagne[58] monitored *t*BuONa/ArONa mixtures (Ar = 4-*tert*-butylphenyl) by ^{1}H NMR. They resolved $(t\text{BuONa})_m(\text{ArONa})_n$ tetramers (Scheme 3; equations implic-

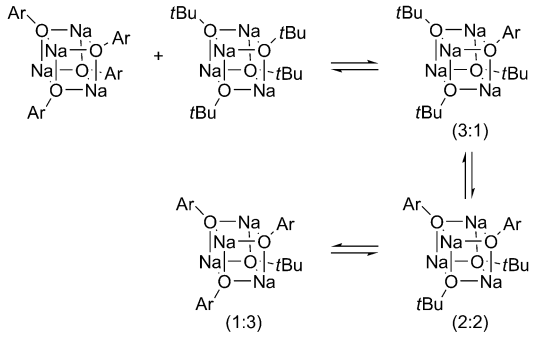

Scheme 3.

itly balanced). Although they stopped short of an actual Job plot, this work stands out by exploiting the characteristics of the ensemble of heteroaggregates to support the assignment of the *homoaggregates*.

In 2004, we chanced upon an ensemble generated from a mixture of *R* and *S* β-amino ester enolates [Eq. (40)] shown using MCV to be hexamers.[53]

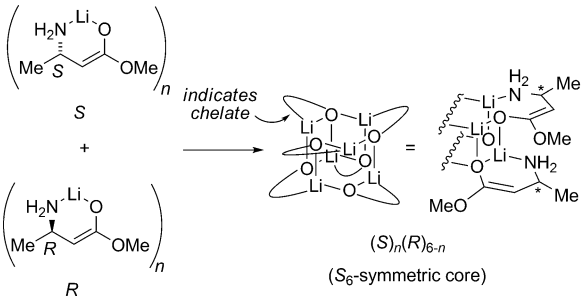

(40)

In theory, the hexamer-based Job plot should resemble that in Figure 9; however, because of the enantiomeric pairings of aggregates—$\mathbf{R}_6/\mathbf{S}_6$, $\mathbf{RS}_5/\mathbf{R}_5\mathbf{S}$, and $\mathbf{R}_2\mathbf{S}_4/\mathbf{R}_4\mathbf{S}_2$—constituting four pairs of indistinguishable mirror images, plotting the hexamers versus mole fraction afforded four distinguishable forms (Figure 10).[53a] Iterative least-squares fit provided direct measures of significant deviations from a statistical distribution. Subsequent studies of structurally distinct β-amino ester enolates showed the full seven-aggregate ensembles (Figure 9).[53d]

We had been seeking a general solution to the problem of determining the aggregation state of lithium enolates and related O-lithiated species for many years; ensembles of

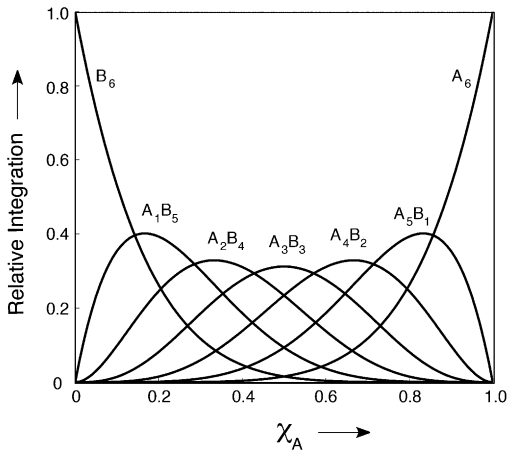

Figure 9. Job plot showing a statistical ensemble of hexamers in which all forms can be observed [Eq. (35), $n=6$].[53d]

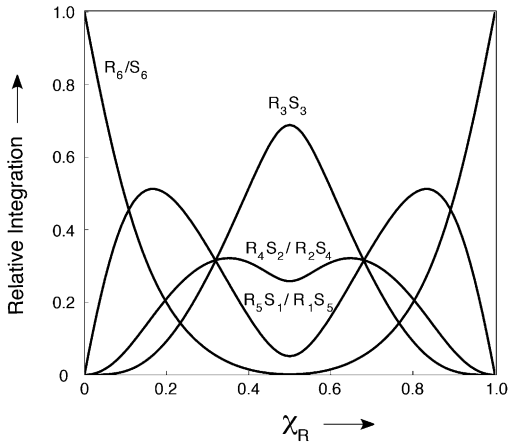

Figure 10. Job plot showing the ensemble of hexamers derived from *R* and *S* β-aminoester enolates [Eq. (40)]. The significant deviation from statistical favoring the $\mathbf{R_3S_3}$ hexamer causes the minimum in the $\mathbf{R_4S_2}$/$\mathbf{R_2S_4}$ curve to be visible.

homo- and heteroaggregates in conjunction with MCV provided this solution. We subsequently determined the aggregation states of more than 100 ROLi/solvent combinations. Although dimers and tetramers are the most prevalent,[59] all possible aggregation states through hexamer have been identified (Figure 11).[60]

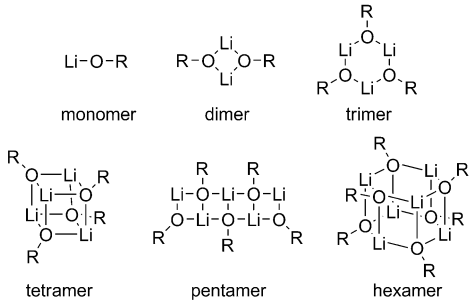

Figure 11.

4.4. Job Plots and Reaction Kinetics

Most applications of MCV focus on observable complexation—the ground state. Rate laws, in conjunction with detailed understanding of reactant structures, provide the stoichiometries of the rate-limiting transition structures.[61] Accordingly, Job plots in which the measured physical property, *P*, is some variant of rate (initial rates or observed rate constants) provide relative stoichiometries of rate-limiting transition structures.[10,26,32,62,65] The only researchers to fully embrace Job plots as kinetic probes are the bioinorganic chemists interested in modeling metal-catalyzed hydrolyses.[63,64] A series of papers by Ming and Zhao[64l,o] are notable for their rigorous data analysis to examine changing mechanisms and high-order *n*:*n* stoichiometries of rate-limiting transition structures.

A particularly simple model of hydrolytic enzymes by Prince and Wooley[63] examined the hydration of acetaldehyde in the presence of zinc and acetate anions [Eq. (41)]. Nonlinear plots of $ZnOAc_2$ concentration versus k_{obsd} suggested cooperativity. A Job plot showed the stoichiometry of the rate-limiting transition structure in acetate anions (k_{obsd} versus $X_{acetate}$). Simulations of the Job plot examined mechanisms involving first, second, and mixed orders in acetate anion. The mixed-order pathway gave the best fit. This fitting protocol allowed the rate constants to be extracted directly from the Job plots. A slightly more nuanced enzyme model reported by Jiang and co-workers[64a] and illustrated in Equation 42 demonstrated that the active catalyst in a pyridyl ester hydrolysis was a 1:1 species in the hydrolysis.

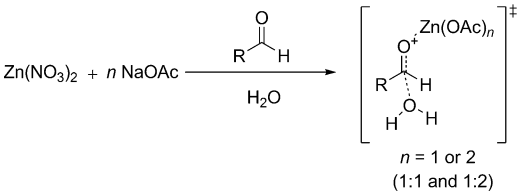

(41)

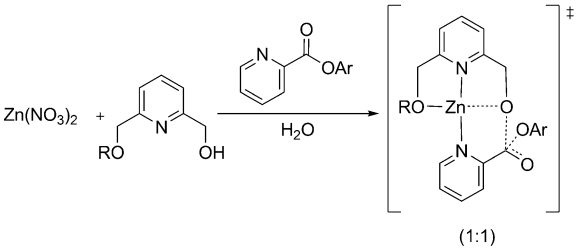

(42)

We have had several occasions to use MCV to examine autocatalysis in reactions of lithium diisopropylamide [LDA; Eq. (43)].[32] The autocatalysis was traced to a rate-limiting condensation of LDA with the resulting aryllithium in a 2:2 stoichiometry. The resulting Job plot showed a characteristic bell shape akin to that in Figure 4 (canted by the basal rate of the uncatalyzed pathway). The maximum at $X_A = 0.50$ stems from using normality rather than aggregate molarity. A fit to the simple general expression in Equation (8) was valid

because of the low steady-state concentration of the mixed aggregate.[65]

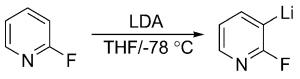

(43)

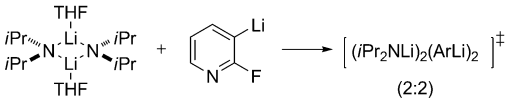

(44)

4.5. Job Plots and Reaction Coordinates

Examples of MCV being used to investigate association in rate-limiting transition structures are rare, yet we see enormous potential. In a particularly powerful application of MCV, insights into both ground state and transition state associations can be obtained from a single plot.

Imagine ligand-dependent reaction rates as illustrated generically in Equations (45) and (46). Ligands L_1 and L_2 could be traditional ligands such as a phosphines or something more fleeting such as a coordinating solvent. The ligand-dependent reactions could afford the same product at different rates or form different products. In an altogether different setting, L_1 and L_2 could represent two substrates reacting with a common enzyme.

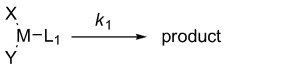

(45)

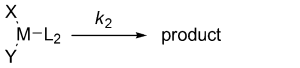

(46)

What is the origin of the relative rates? To answer this question, we reframe the reaction as shown in Scheme 4 and present the underlying thermochemistry in Scheme 5. How do we describe the relative reactivities in terms of the activation energies ($\Delta G^{\ddagger}_1$ and $\Delta G^{\ddagger}_2$) and the relative energies of the ground states (ΔG°_{GS}) and transition states (ΔG°_{TS})?

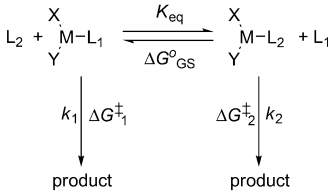

Scheme 4.

MCV offers a remarkably simple solution. The total ligand concentration is kept constant, and k_{obsd} is measured versus mole fraction of L_2 (X_{L2}).[66] Rate constants k_1 and k_2 (corresponding to $\Delta G^{\ddagger}_1$ and $\Delta G^{\ddagger}_2$) and K_{eq} (corresponding to ΔG°_{GS}) are adjustable parameters available through nonlinear least squares fit to Equation (47).

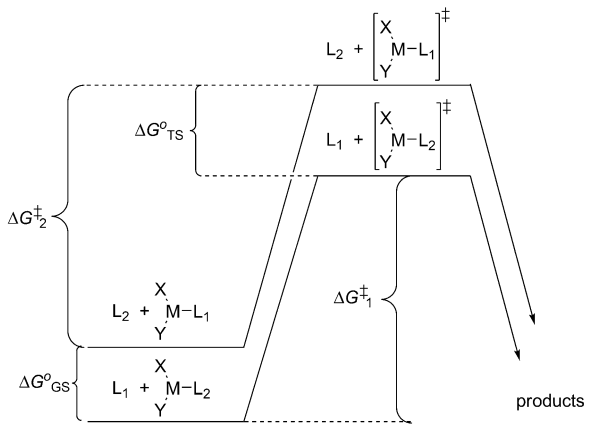

Scheme 5.

$$k_{obsd} = \frac{k_2 X_{L_2} + k_1 K_{eq}(1 - X_{L_2})}{X_{L_2} + K_{eq}(1 - X_{L_2})} \quad (47)$$

Figure 12 illustrates simulated Job plots corresponding to a k_{rel} value of 10 ($k_2 = 10k_1$) and different values of K_{eq}. Note that the optimized stoichiometry—exclusively L_2—is still indicated by the maximum in the curve, but the maximum corresponds to the right-hand y intercept. Nonlinear least squares fit to Equation (47) readily affords the values of k_1, k_2, and K_{eq}.

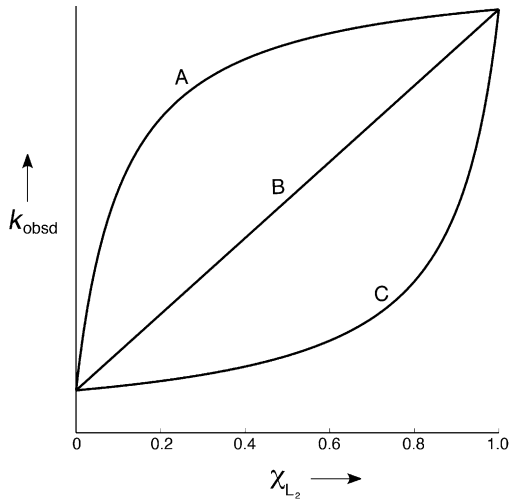

Figure 12. Theoretical curves corresponding to Scheme 5 in which y intercepts reflect a 10-fold greater reactivity of M-L_2 relative to M-L_1 [$k_2/k_1 = 10$; Eq. (47)]. The curves derive from differential binding of L_1 and L_2: Curve A: strong binding of L_2 relative to L_1 ($K_{eq} = 10$); curve B: equal binding of L_1 and L_2 ($K_{eq} = 1.0$); curve C: strong binding of L_1 relative to L_2 ($K_{eq} = 0.1$).

The three limiting cases of interest are as follows:

Curve A. Correlation of strong ligation in the ground state ($K_{eq} = 10$) with higher overall reactivity shows the rates rising at relatively low proportions of L_2 and saturating. The higher rates for L_2 stem from stabilization at the rate-limiting transition state that necessarily exceeds the stabilization in the ground state ($\Delta G^{\circ}_{GS} < \Delta G^{\circ}_{TS}$):

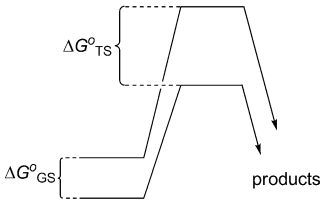

Curve B. Equivalent binding of L_1 and L_2 in the ground state ($K_{eq} = 1.0$) causes a linear rise in rates with mole fraction ($\Delta G°_{TS} > \Delta G°_{GS} = 0$):

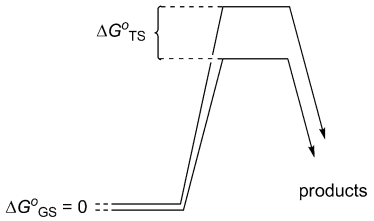

Curve C. Correlation of *weak* ligation of L_2 ($K_{eq} = 0.1$) with high reactivity shows rates rise markedly only at high L_2 mole fraction (Figure 12). The accelerations are traced to differential stabilization in the ground state ($\Delta G°_{GS} > \Delta G°_{TS}$):

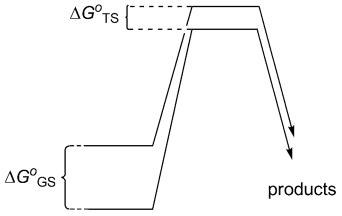

Gleaning such rich thermochemical information from a single plot is highly desirable. We know of only a handful of examples, however, and they emanate from our laboratory. Three are instructive.[66]

Ketone enolizations by lithium hexamethyldisilazide solvated by trialkylamines [Eq. (48)] are highly sensitive to the steric demands of the amine, displaying rates spanning a 3000-fold range.[66b,e]

Rate studies revealed a mechanism via a dimer-based transition structure (Scheme 6). MCV showed that the accelerations correlate inversely with the binding constant

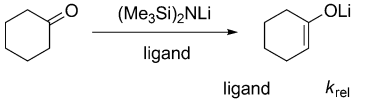

ligand	k_{rel}
none	1.0
Me_2NEt	200
Et_3N	3000

(48)

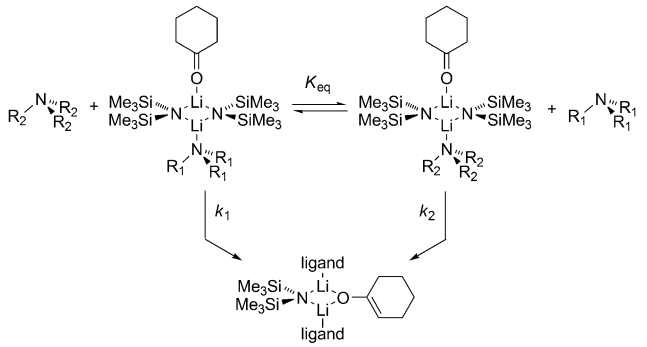

Scheme 6.

of the ligand but do not involve ligand dissociation. Contrary to conventional wisdom, however, a Job plot showing a curve analogous to curve C in Figure 12 indicates ground state destabilization. Multiple examples revealed a surprising linear free energy relationship in which $\Delta G°_{TS} \approx 0.6 \Delta G°_{GS}$.[66e]

Snieckus-Fries rearrangement of an LDA-ArLi mixed dimer in dimethoxyethane (DME) was 90 times faster than in *n*BuOMe [Eq. (49)].[66c]

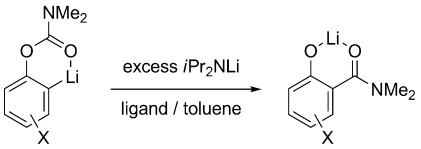

(49)

A Job plot derived by monitoring rates versus solvent mole fractions afforded a nearly linear curve analogous to curve B in Figure 12. The acceleration derives from exclusively transition state stabilization ($\Delta G°_{GS} = 0$) owing to chelation by DME only in the rate-limiting transition structure. DME is said to be "hemilabile" (Scheme 7).

Hemilability in organolithium chemistry can elicit profound accelerations owing to selective stabilization at the

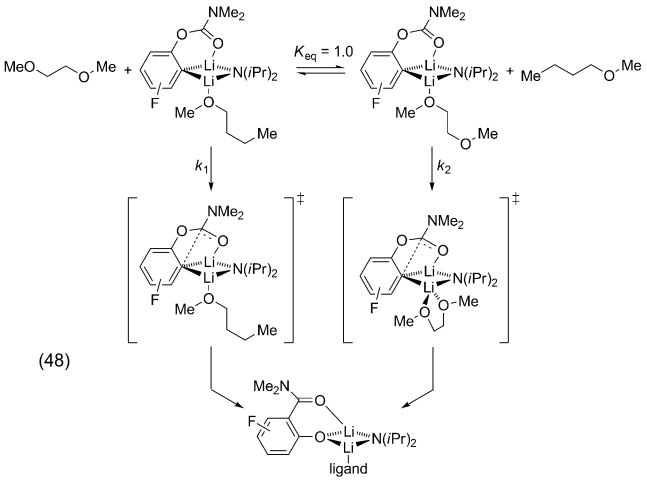

Scheme 7.

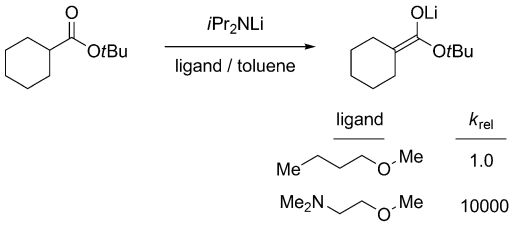

(50)

transition structure. The most striking example is illustrated in Equation (50) and Scheme 8.[66e] Once again, a Job plot in which rate constants are monitored versus solvent mole

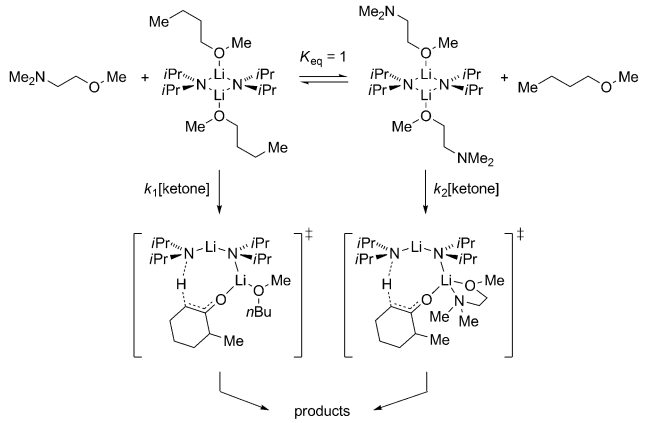

Scheme 8.

fraction traces the 10000-fold acceleration to η^1 coordination in the ground state ($\Delta G°_{GS} = 0$) and η^2 coordination in the rate-limiting transition state ($\Delta G°_{TS} = 3$–4 kcal mol^{-1}). The double substitution and affiliated second-order ligand dependence impart a distinct sigmoidal shape in the Job plot (Figure 13).

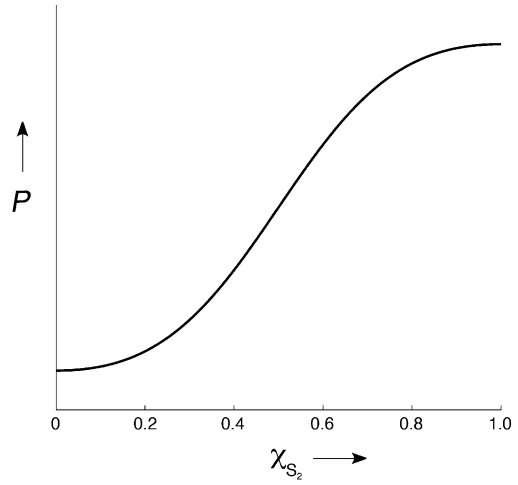

Figure 13. Simulated Job plot for the scenario in Scheme 8 in which a double ligand substitution elicits sigmoidal curvature according to Equation (51).[66e]

$$k_{obsd} = \frac{k_1(1 - X_{S_2})^2 + k_2 K_{eq} X_{S_2}^2}{(1 - X_{S_2})^2 + X_{S_2}^2}$$

5. Conclusions

At the outset, we intended to make MCV accessible to those unfamiliar with the method and, more specifically, broaden its user base within organometallic community. A survey of thousands of papers, however, revealed applications of MCV within organometallic chemistry are remarkably rare. Case studies with a decidedly more inorganic flavor augment key underlying principles and the potential potency of the method.

We also were surprised by some of the mathematical subtleties, which partially explain why data analysis using least squares best-fit protocols are extraordinarily rare.[3,25–29,33] In short, relatively few researchers fit the data to a model and, in our opinion, those who do have not made it especially easy to understand for those who do not.

We find it especially useful to monitor not only the concentration of the associated complex, $\mathbf{A}_m\mathbf{B}_n$, but also the disappearance of the two components, **A** and **B**. Monitoring all species provides a direct measure of concentration—a normalized *y* axis—that, in turn, allows extraction of the association constant, K_{eq}.

Applications of MCV using some variant of rate as the observable is profoundly underused. It seems as though only the ester and phosphate ester hydrolysis community seem to fully appreciate MCV. This blind spot in other disciplines is especially notable given that MCV provides a shortcut to stoichiometries of rate-limiting transition structures that is particularly accessible to those not well schooled in reaction kinetics per se.

Some of the most complex applications of MCV are found in the chemistry of ensembles. Clearly, those interested in serial (multi-site) substitutions and aggregations would benefit from MCV.

In the final section of the review, we showed an application of MCV that provides thermochemical insights into the reaction coordinate—a description of the origins of rate differences in terms of relative ground state and transition state energetic differences—using a single plot of rate constant versus mole fraction. Although we have used this seemingly obvious strategy on a half dozen occasions, we cannot find analogous cases. Existant cases may surface on account of this review, and we hope that new applications will emerge.

In summary, despite 80 years of development leading to some remarkably rigorous and scholarly analyses, MCV has considerable room to expand its role in the study of association phenomena in chemistry and biochemistry.

6. Literature Search Protocol

Although the scope of this review is limited to a discussion of the applications of MCV in organometallic chemistry, an extensive search of the literature was conducted using a multi-

tiered search. JabRef allowed us to consolidate the references from all searches and remove the redundancies, affording > 6500 publications. The core search was conducted in *Web of Science*. Search terms included "method of continuous variation," "method of continuous variations," "Job plot," "Job plots," and "Job's plot." Additional *Web of Science* citation searches were carried out on the original reference of Job,[2] the primary reviews deemed central to the field,[24,26–28,29c] and the other significant papers. In some cases the journals were deemed sufficiently remote from organometallic chemistry and from the usual Job plot citations that they were excluded. In other instances, we detected gaps emanating from specific publishing houses and publishing years. Accordingly, we also used the searching algorithms of the American Chemical Society, Royal Society of Chemistry, Wiley, Elsevier, and Springer to augment the existing database. We manually perused papers to check for citations missed by the electronic searching protocols. Unavailable publications were not pursued unless deemed germane from the limited available information.

Note added in proof: Several papers germane to the this Review have appeared since completion of the search. These include the application of MCV to a metal-catalyzed dehydrogenative C–N bond formation,[67] a Rh-catalyzed hydroacylation,[68] organometallic associations with cyclodextrins,[69] and coordination of pincer ligands to Pd.[70]

We thank the National Institutes of Health (GM077167) for direct support of this work, Leah McEwen for extensive help with construction of the literature search, and Dr. Marshall Hayes for help with some translations.

Received: May 14, 2013
Published online: October 24, 2013

[1] a) I. Ostromisslensky, *Ber. Dtsch. Chem. Ges.* **1911**, *44*, 268 – 273; b) O. Ruff, *Z. Phys. Chem.* **1911**, *76*, 21 – 57; c) R. B. Denison, *Trans. Faraday Soc.* **1912**, *8*, 20 – 34; d) E. Cornec, G. Urbain, *Bull. Soc. Chim.* **1919**, *25*, 215 – 222.
[2] P. Job, *Ann. Chim.* **1928**, *9*, 113 – 203.
[3] S. E. Hayes, *J. Chem. Educ.* **1995**, *72*, 1029 – 1031.
[4] M. T. Beck, I. Nagypál, *Chemistry of Complex Equilibria*, *2nd ed.*, Ellis Horwood, New York, **1990**.
[5] F. R. Hartley, J. L. Wagner, *J. Organomet. Chem.* **1973**, *55*, 395 – 403.
[6] J. H. Espenson, *Chemical Kinetics and Reaction Mechanisms*, *2nd ed.*, McGraw-Hill, New York, **1995**.
[7] a) G. Scatchard, *Ann. N. Y. Acad. Sci.* **1949**, *51*, 660 – 672; b) For a comparison of methods for the determination of association constants from solution NMR data see: L. Fielding, *Tetrahedron* **2000**, *56*, 6151 – 6170.
[8] a) K. S. Klausen, F. J. Langmyhr, *Anal. Chim. Acta* **1963**, *28*, 335 – 340; b) K. S. Klausen, F. Langmyhr, *Anal. Chim. Acta* **1968**, *40*, 167 – 169; c) K. S. Klausen, *Anal. Chim. Acta* **1969**, *44*, 377 – 384.
[9] T. Doiuchi, Y. Minoura, *Macromolecules* **1978**, *11*, 270 – 274.
[10] a) T. Doiuchi, H. Yamaguchi, Y. Minoura, *Eur. Polym. J.* **1981**, *17*, 961 – 968; b) J. M. G. Cowie, S. H. Cree, R. Ferguson, *Eur. Polym. J.* **1989**, *25*, 737 – 743.
[11] J. F. Tate, M. M. Jones, *J. Inorg. Nucl. Chem.* **1960**, *12*, 241 – 251.
[12] T. L. Brown, R. L. Gerteis, D. A. Bafus, J. A. Ladd, *J. Am. Chem. Soc.* **1964**, *86*, 2135 – 2141.
[13] Y. L. Loukas, *J. Pharm. Pharmacol.* **1997**, *49*, 944 – 948.
[14] C. C. Addison, J. C. Sheldon, B. C. Smith, *J. Chem. Soc. Dalton Trans.* **1974**, 999 – 1002.
[15] a) K. Adachi, H. Watarai, *Chem. Eur. J.* **2006**, *12*, 4249 – 4260; b) H. Goto, Y. Okamoto, E. Yashima, *Chem. Eur. J.* **2002**, *8*, 4027 – 4036.
[16] F. Yan, R. Copeland, H. G. Brittain, *Inorg. Chim. Acta* **1983**, *72*, 211 – 216.
[17] J. Fenger, K. E. Siekierska, B. S. Jensen, *J. Inorg. Nucl. Chem.* **1971**, *33*, 4366 – 4368.
[18] E. L. Que, E. Gianolio, S. L. Baker, A. P. Wong, S. Aime, C. J. Chang, *J. Am. Chem. Soc.* **2009**, *131*, 8527 – 8536.
[19] T. Ouhadi, A. Hamitou, R. Jerome, P. Teyssie, *Macromolecules* **1976**, *9*, 927 – 931.
[20] Addition of a 10-fold volume of a solution of substrate **A** to a small volume of an equimolar solution of **B** by an automated flow system will provide a continuously changing **A** and **B** proportion while maintaining the sum of **A** and **B** at fixed concentration. The net effect is an automated change of X_A from 1.0 to 0.10. P. MacCarthy, *Anal. Chem.* **1978**, *50*, 2165.
[21] A. Sayago, M. Boccio, A. G. Asuero, *Int. J. Pharm.* **2005**, *295*, 29 – 34.
[22] J. H. Bell, R. F. Pratt, *Inorg. Chem.* **2002**, *41*, 2747 – 2753.
[23] D. B. Collum, A. J. McNeil, A. Ramirez, *Angew. Chem.* **2007**, *119*, 3060 – 3077; *Angew. Chem. Int. Ed.* **2007**, *46*, 3002 – 3017.
[24] E. Bruneau, D. Lavabre, G. Levy, J. C. Micheau, *J. Chem. Educ.* **1992**, *69*, 833 – 837.
[25] E. J. Olson, P. Bühlmann, *J. Org. Chem.* **2011**, *76*, 8406 – 8412.
[26] C. Y. Huang, *Methods Enzymol.* **1982**, *87*, 509 – 525.
[27] V. M. S. Gil, N. C. Oliveira, *J. Chem. Educ.* **1990**, *67*, 473 – 478.
[28] K. Hirose, *J. Inclusion Phenom. Macrocyclic Chem.* **2001**, *39*, 193 – 209.
[29] a) C. A. Schalley, *Analytical Methods in Supramolecular Chemistry*, Wiley-VCH, Weinheim, **2007**; b) K. A. Connors, *Binding Constants*: *The Measurement of Molecular Complex Stability*, Wiley, New York, **1987**; c) W. Likussar, D. F. Boltz, *Anal. Chem.* **1971**, *43*, 1265 – 1272; d) F. J. C. Rossotti, H. Rossotti, *The Determination of Stability Constants*, McGraw-Hill, New York, **1961**.
[30] Bühlmann and coworkers have a typo in their version of Equation (5),[25] which does not detract from the overall importance or rigor of their analyses.
[31] M. A. Jacobson, I. Keresztes, P. G. Williard, *J. Am. Chem. Soc.* **2005**, *127*, 4965 – 4975.
[32] L. Gupta, A. C. Hoepker, Y. Ma, M. S. Viciu, M. F. Faggin, D. B. Collum, *J. Org. Chem.* **2013**, *78*, 4214 – 4230.
[33] a) E. Asmus, *Z. Anal. Chem.* **1961**, *183*, 321 – 333; b) E. Asmus, *Z. Anal. Chem.* **1961**, *183*, 401 – 412.
[34] S. O. Kang, V. M. Lynch, V. W. Day, E. V. Anslyn, *Organometallics* **2011**, *30*, 6233 – 6240.
[35] A. S. McCall, H. Wang, J. M. Desper, S. Kraft, *J. Am. Chem. Soc.* **2011**, *133*, 1832 – 1848.
[36] I. M. Baibich, A. Parlier, H. Rudler, *J. Mol. Catal.* **1989**, *53*, 193 – 202.
[37] L. Du, P. Cao, J. Xing, Y. Lou, L. Jiang, L. Li, J. Liao, *Angew. Chem.* **2013**, *125*, 4301 – 4305; *Angew. Chem. Int. Ed.* **2013**, *52*, 4207 – 4211.
[38] T. E. Geswindt, W. J. Gerber, H. E. Rohwer, K. R. Koch, *Dalton Trans.* **2011**, *40*, 8581 – 8588.
[39] S. B. Colbran, B. H. Robinson, J. Simpson, *Organometallics* **1985**, *4*, 1594 – 1601.
[40] R. Kania, K. Lewinski, B. Sieklucka, *Dalton Trans.* **2003**, 1033 – 1040.
[41] Sulfur dioxide complexation to rhodium and iridium have been used to model CO complexation central to hydroformylation;

a) A. Wojcicki, *Adv. Organomet. Chem.* **1974**, *12*, 31 – 81; b) M. F. Joseph, M. C. Baird, *Inorg. Chim. Acta* **1985**, *96*, 229 – 230.

[42] G. N. Salaita, F. H. Jumean, N. W. Mulki, *Inorg. Chim. Acta* **1978**, *26*, 221 – 222.

[43] Z. Rozwadowski, S. Malik, G. Toth, T. Gati, H. Duddeck, *Dalton Trans.* **2003**, 375 – 379.

[44] K. Yamamoto, S. Nakazawa, A. Matsufuji, T. Taguchi, *J. Chem. Soc. Dalton Trans.* **2001**, 251 – 258.

[45] G. A. Catton, F. A. Hart, G. P. Moss, *J. Chem. Soc. Dalton Trans.* **1976**, 208 – 210.

[46] J. T. Sheff, A. L. Lucius, S. B. Owens, G. M. Gray, *Organometallics* **2011**, *30*, 5695 – 5709.

[47] D. Lee, C. L. Williamson, L. Chan, M. S. Taylor, *J. Am. Chem. Soc.* **2012**, *134*, 8260 – 8267.

[48] H. Hamaki, N. Takeda, T. Yamasaki, T. Sasamori, N. Tokitoh, *J. Organomet. Chem.* **2007**, *692*, 44 – 54.

[49] P. J. Pospisil, S. R. Wilson, E. N. Jacobsen, *J. Am. Chem. Soc.* **1992**, *114*, 7585 – 7587.

[50] J. J. Eisch, S. G. Rhee, *J. Organomet. Chem.* **1972**, *42*, C73 – C76.

[51] H. Weingarten, J. R. Van Wazer, *J. Am. Chem. Soc.* **1965**, *87*, 724 – 730.

[52] L. C. D. Groenweghe, J. R. Van Wazer, A. W. Dickinson, *Anal. Chem.* **1964**, *36*, 303 – 307.

[53] a) A. J. McNeil, G. E. S. Toombes, S. V. Chandramouli, B. J. Vanasse, T. A. Ayers, M. K. O'Brien, E. Lobkovsky, S. M. Gruner, J. A. Marohn, D. B. Collum, *J. Am. Chem. Soc.* **2004**, *126*, 5938 – 5939; b) A. J. McNeil, G. E. S. Toombes, S. M. Gruner, E. Lobkovsky, D. B. Collum, S. V. Chandramouli, B. J. Vanasse, T. A. Ayers, *J. Am. Chem. Soc.* **2004**, *126*, 16559 – 16568; c) A. J. McNeil, D. B. Collum, *J. Am. Chem. Soc.* **2005**, *127*, 5655 – 5661; d) L. R. Liou, A. J. McNeil, G. E. S. Toombes, D. B. Collum, *J. Am. Chem. Soc.* **2008**, *130*, 17334 – 17341.

[54] P. Goralski, D. Legoff, M. Chabanel, *J. Organomet. Chem.* **1993**, *456*, 1 – 5.

[55] P. Goralski, M. Chabanel, *Inorg. Chem.* **1987**, *26*, 2169 – 2171.

[56] D. P. Novak, T. L. Brown, *J. Am. Chem. Soc.* **1972**, *94*, 3793 – 3798.

[57] S. Desjardins, K. Flinois, H. Oulyadi, D. Davoust, C. Giessner-Prettre, O. Parisel, J. Maddaluno, *Organometallics* **2003**, *22*, 4090 – 4097.

[58] R. M. Kissling, M. R. Gagne, *J. Org. Chem.* **2001**, *66*, 9005 – 9010.

[59] a) L. R. Liou, A. J. McNeil, A. Ramirez, G. E. S. Toombes, J. M. Gruver, D. B. Collum, *J. Am. Chem. Soc.* **2008**, *130*, 4859 – 4868; b) J. M. Gruver, L. R. Liou, A. J. McNeil, A. Ramirez, D. B. Collum, *J. Org. Chem.* **2008**, *73*, 7743 – 7747.

[60] a) T. S. De Vries, A. Goswami, L. R. Liou, J. M. Gruver, E. Jayne, D. B. Collum, *J. Am. Chem. Soc.* **2009**, *131*, 13142; b) L. L. Tomasevich, D. B. Collum, *J. Org. Chem.* **2013**, *78*, 7498 – 7507; c) For additional application of MCV to polylithiated lithium phenolates, see H. Nakajima, M. Yasuda, A. Baba, *Dalton Trans.* **2012**, *41*, 6602 – 6606.

[61] Rate laws, in conjunction with knowledge of the reactants, provide the stoichiometries of the rate-limiting transition structures.

[62] A. P. Jamakhandi, P. Kuzmic, D. E. Sanders, G. P. Miller, *Biochemistry* **2007**, *46*, 10192 – 10201.

[63] R. H. Prince, P. R. Wooley, *J. Chem. Soc. Dalton Trans.* **1972**, 1548 – 1554.

[64] a) Y. Song, X. Han, X. Guo, Q. Zeng, F. Jiang, *Colloids Surf. A* **2011**, *392*, 110 – 115; b) H.-Y. Jiang, C.-H. Zhou, K. Luo, H. Chen, J.-B. Lan, R. G. Xie, *J. Mol. Catal. A* **2006**, *260*, 288 – 294; c) T. A. Lönnberg, M. Helkearo, A. Janscó, T. Gajda, *Dalton Trans.* **2012**, *41*, 3328 – 3338; d) J.-S. You, X.-Q. Yu, X.-Y. Su, T. Wang, Q.-X. Xiang, M. Yang, R.-G. Xie, *J. Mol. Catal. A* **2003**, *202*, 17 – 22; e) A. Benjelloun, P. Lochon, A. Brembilla, *J. Mol. Catal. A* **1999**, *140*, 215 – 223; f) V. Faivre, A. Brembilla, P. Lochon, *J. Mol. Catal.* **1993**, *85*, 45 – 56; g) J. Budka, F. Hampl, F. Liska, P. Scrimin, P. Tecilla, U. Tonellato, *J. Mol. Catal. A* **1996**, *104*, L201 – L203; h) L.-G. Qiu, A.-J. Xie, Y.-H. Shen, *J. Mol. Catal. A* **2006**, *244*, 58 – 63; i) J. Fubin, J. Bingying, C. Yong, Y. Xiaoqi, Z. Xiancheng, *J. Mol. Catal. A* **2004**, *210*, 9 – 16; j) S. Bhattacharya, K. Snehalatha, V. P. Kumar, *J. Org. Chem.* **2003**, *68*, 2741 – 2747; k) T. Fujita, Y. Inaba, K. Ogino, W. Tagaki, *Bull. Chem. Soc. Jpn.* **1988**, *61*, 1661 – 1667; l) Q.-X. Xiang, X.-Q. Yu, X.-Y. Su, Q.-S. Yan, T. Wang, J.-S. You, R.-G. Xie, *J. Mol. Catal. A* **2002**, *187*, 195 – 200; m) L. Wang, Y. Ye, V. Lykourinou, A. Angerhofer, L.-J. Ming, Y. Zhao, *Eur. J. Inorg. Chem.* **2011**, 674 – 682; n) F. Mancin, P. Tecilla, U. Tonellato, *Langmuir* **2000**, *16*, 227 – 233; o) V. Lykourinou, A. I. Hanafy, K. S. Bisht, A. Angerhofer, L.-J. Ming, *Eur. J. Inorg. Chem.* **2009**, 1199 – 1207.

[65] For a related case in which simplified Equation (8) was used to *approximate* a fit of observable $\mathbf{A}_m\mathbf{B}_n$ complexation, see: Y. Ma, A. C. Hoepker, L. Gupta, M. F. Faggin, D. B. Collum, *J. Am. Chem. Soc.* **2010**, *132*, 15610 – 15623.

[66] a) M. P. Bernstein, D. B. Collum, *J. Am. Chem. Soc.* **1993**, *115*, 8008 – 8018; b) P. Zhao, B. L. Lucht, S. L. Kenkre, D. B. Collum, *J. Org. Chem.* **2004**, *69*, 242 – 249; c) J. C. Riggs, K. J. Singh, Y. Ma, D. B. Collum, *J. Am. Chem. Soc.* **2008**, *130*, 13709 – 13717; d) J. F. Remenar, D. B. Collum, *J. Am. Chem. Soc.* **1997**, *119*, 5573 – 5582; e) P. Zhao, D. B. Collum, *J. Am. Chem. Soc.* **2003**, *125*, 14411 – 14424; f) A. Ramírez, E. Lobkovsky, D. B. Collum, *J. Am. Chem. Soc.* **2003**, *125*, 15376.

[67] L.-M. Louillat, F. W. Patureau, *Org. Lett.* **2013**, *15*, 164 – 167.

[68] J.-W. Park, J.-H. Park, C.-H. Jun, *J. Org. Chem.* **2008**, *73*, 5598 – 5601.

[69] C Blaszkiewicz, H. Bricout, E. Leonard, C. Len, D. Landy, C. Cezard, F. D. Pilard, E. Monfliera, S. Tilloy, *Chem. Commun.* **2013**, *49*, 6989 – 6991.

[70] M. Q. Slagt, J. T. B. H. Jastrzebski, R. J. M. K. Klein Gebbink, H. J. van Ramesdonk, J. W. Verhoeven, D. D. Ellis, A. L. Spek, G. van Koten, *Eur. J. Org. Chem.* **2003**, 1692 – 1703.